PUB-77-135-E
T 0008

Nucl. Phys. B.
FERMILAB-PUB-77-135-E

INCLUSIVE PRODUCTION OF NEUTRAL STRANGE PARTICLES AT 300 GeV: TRIPLE REGGE BEHAVIOR

by

T. Devlin, B. Edelman, R. T. Edwards, J. Norem*,

L. Schachinger and P. Yamin†

Physics Department‡
Rutgers - The State University
New Brunswick, New Jersey 08903

G. Bunce, R. Handler, R. March, P. Martin

L. Pondrom and M. Sheaff

Physics Department††
University of Wisconsin
Madison, Wisconsin 53706

K. Heller, O. E. Overseth, and P. Skubic

Physics Department‡
University of Michigan
Ann Arbor, Michigan 48109

Abstract

The process p + nucleon → V° + anything has been studied at 300 GeV for V° = Λ°, $\bar{\Lambda}^\circ$, and K_s°. The data are consistent with a simple Mueller-Regge formulation in the appropriate limit. Values of $\alpha(t)$ computed from the data agree with those expected from the simplest triple-Regge diagrams. If the Pomeron is not a pure SU(3) singlet, a similar diagram is consistent with the Feynman x-dependence of the observed polarization of inclusively produced Λ°.

We have obtained data on inclusive production of Λ°, K_s°, and $\bar{\Lambda}^\circ$ by 300 GeV protons in the Fermilab Neutral Hyperon Beam. At angles from 0 to 9 milliradians, and in the higher range of Feynman x, the invariant cross sections converge to a single-term triple-Regge behavior. Fits to the data yield values of $\alpha(t)$ consistent with K* (K**) exchange, with Σ exchange, and with Regge-like behavior of a strange di-baryon system for Λ°, K_s° and $\bar{\Lambda}^\circ$ respectively. Interference between K* and K** exchange is consistent with the Feynman x-dependence of the Λ° polarization observed in the same data.[1] In order for the triple-Regge representation of this interference to have a non-zero contribution, the Pomeron cannot be a pure SU(3) singlet. Absorptive corrections may also play a role in the polarization.

Measurements were made in the Neutral Hyperon Beam at Fermilab. Protons at 300 GeV were steered onto our production target at an angle which could be varied from 0 to 10 milliradians. A magnetized beam channel removed charged particles and collimated the neutral beam to about 1 milliradian divergence and 10 mm diameter. The neutral strange particles were detected by their decays into two charged particles. A magnetic-spectrometer and multi-wire-proportional-chamber system of conventional design was used to detect the two charged decay products. The wire-chamber data were reconstructed to determine the invariant mass of the parent neutral particle under various hypotheses for the charged-particle masses. Cuts on the data were made to eliminate ambiguous events and backgrounds. For each laboratory angle setting, and for each momentum bin, corrections were made for decay probability,

spectrometer acceptance, target-out background and several other minor experimental effects. Results are expressed as $E\, d^3\sigma/dp^3$ vs. momentum for each production angle, produced particle and production target. More detailed accounts of the apparatus, analysis and data are presented elsewhere.[1,2]

For this study, we have used a representative sub-sample of the whole data set: Be, and Pb targets at production angles of 0.6, 1.4, 3.1, 5.0, 7.1 and 8.9 mr; and a Cu target at 0.6, 1.4 and 8.9 mr. We have further restricted our attention to the higher range of x values available to us for reasons discussed below.

The process under consideration is $a + b \rightarrow c + d$, where a is a proton, b is a nucleon (after correction for nuclear effects), c is a V° (Λ°, $\bar{\Lambda}^\circ$ or K_s°), and d is some unobserved multi-particle system. We use the following kinematic quantities: $s = |p_a + p_b|^2$; $t = |p_a - p_c|^2$; $M^2 = M_d^2 = |p_a + p_b - p_c|^2$; $\nu = M^2 - t - M_b^2$; and $x = 2\, p_{cz}/s^{1/2}$, where p_{cz} is the longitudinal component of p_c in the c.m. system. We define ν_1 and ν_0 as the maximum and minimum values of ν, and we use as a kinematic variable the quantity $(\nu - \nu_0)/(\nu_1 - \nu_0)$ which is equal to $(1 - x)$ and to M^2/s to an excellent approximation at 300 GeV. This variable is appropriate for use in triple Regge analyses[3], and is exactly zero at the kinematic limit. Hereafter, we use (1-x) to refer to it.

The data for the Be target are shown in Fig. 1. (The Cu, Pb and extrapolated single-nucleon results[2], aside from an overall factor, appear very similar.)

For $x > 0.6$, we have compared our Λ° and K_s° results with low energy data[4] in order to study the s-dependence.[2] If non-scaling terms behave like $s^{-1/2}$, then less than 20% of the high-x cross section at 300 GeV is due to such terms. There is less evidence to support scaling for $\bar{\Lambda}^\circ$. We proceed under the assumption that scaling is approximately true.

Functions of the form

$$\sigma(x,t)\ |_{\text{fixed }\theta} = E\,\frac{d^3\sigma}{dp^3} = \beta\ (1 - x)^{a(\theta)} \tag{1}$$

give quite good fits to our data. Further, for each type of particle, $a(\theta)$ shows roughly a quadratic dependence on θ. Since t is proportional to θ^2 this is very suggestive of triple-Regge behavior. In such models, the diagram of Fig. 2(a) is used to compute the inclusive cross section for $a + b \to c$ + anything. In cases where α_3 represents a Pomeron, the cross section shows scaling behavior. Further, when $\alpha_1 = \alpha_2 = \alpha$, the contribution of such a diagram to the cross section can be written[3]

$$\alpha(x,t) = \beta(t)\ (1-x)^{[1 - 2\alpha(t)]} \tag{2}$$

Various diagrams relevant to the processes under study here are shown in Fig. 2(b-f).

Unfortunately, much of our data is outside the kinematic region regarded as appropriate for such models, which (at 300 GeV) is roughly $0.02 < (1-x) < 0.2$. We have interpolated our data to determine the (1-x) dependence at fixed t. Fig. 3 shows this for Λ° production from Be. The data show substantial curvature on the log-log scale, and are very poor fits to Eq. 2, except at low

values of (1-x) where the model is expected to be valid or at low t. This excludes direct use of much of our data for Λ° production, and all of that for K° and $\bar{\Lambda}^\circ$ production.

The very simple dependence of the cross section on (1-x) at fixed θ suggests the possibility of extrapolating into the triple-Regge region. If Eq. 1 is true, it is a simple matter to show that

$$1 - 2\,\alpha_i = \lim_{x\to 1} \left.\frac{d[\log\,\sigma(x,t)]}{d[\log\,(1-x)]}\right|_{t=t_i}$$

$$= \left.\frac{d\,\log\,[\sigma(x,t)]}{d\,\log\,[(1-x)]}\right|_{\theta=\theta_i} = a(\theta_i) \qquad (3)$$

where $\alpha_i = \alpha(t_i)$ and $t_i = t(x=1,\ \theta=\theta_i)$. This simply says that, on a log-log scale, the slope at fixed θ converges on the slope at fixed t in the limit x = 1. This relationship allows us to determine the Regge parameter in Eq. 2 from the observed behavior of Eq. 1.

The data from all angles, θ_i, for production of a given particle from a given target were fit simultaneously to a function of the form $\beta_i(1-x)^{(1\,-\,2\alpha_i)}$ where β_i and α_i were the parameters determined by the fit for each specific production angle, θ_i. It should be emphasized that no functional form was forced on the parameters and that there were no constraints favoring particular Regge trajectories.

The various fits had from 26 to 57 data points and six to twelve parameters. All fits had $P(\chi^2)$ between 10% and 70%, except one which was 1%.

In order to extract the single-nucleon results, two methods were used. First, the data were extrapolated to A = 1, then fitted. Second, the individual nuclear cross sections were fitted and the resulting values of α_i extrapolated to A = 1. The $\alpha_i(A)$ were consistent with a weak linear dependence on $A^{1/3}$ as would be expected for double scattering effects in complex nuclei. The agreement between the two methods was generally within statistical errors. Some shift in the kinematic quantities occurs because of Fermi momentum, but this does not affect the values of α_i.

The results for our fits for A = 1 are presented in Table 1, and in Figs. 4-6. The values of β are the intercepts at x = 0, significantly outside the region covered by our data. This results in large statistical errors in cases where the slopes in Fig. 1 are large. For each produced particle, the assumption of constant β is consistent with our data, and the values of α fitted under that assumption vary only slightly from those presented here. Our chief concern is with the behavior of $\alpha(t)$.

We expect the leading diagrams in Λ° production to be those of Fig. 2(b-c). Our measured values of $\alpha(t)$ are plotted in Fig. 4 along with K*(890), K**(1420) and K(494). The connection between our data and the K* and K** states is clear, while the K is not favored. A similar analysis has been performed on Λ° production at 19 GeV.[5] Those results favor values of $\alpha(t)$ lower than ours, and they are more consistent with the K(494). The discrepancy may be due to the difference in energy, or it may be due to the fact that the fits in Ref. 5 were performed at fixed t over a range of x outside the triple-Regge region.

There are a number of Σ states which might contribute to diagrams of the type shown in Fig. 2(d) for K° production. We have plotted some of these in Fig. 5 along with our values of $\alpha(t)$ from K_s° production. It is difficult to single out a specific Σ state for two reasons. First, there may be systematic errors in $\alpha(t)$ because the data lie farther outside the triple-Regge region than in the case of Λ° production. Thus, the extrapolation method may be less accurate. Second, the separation between our values of $\alpha(t)$ and the physical Σ states in Fig. 5 is greater. It is not clear how to join them. However, the general consistency of our data with Σ exchange is obvious, and the usefulness of the model is confirmed.

The production of $\bar{\Lambda}^\circ$ through a diagram like Fig. 2(e) requires the exchange of a di-baryon state of negative strangeness, clearly exotic. No $\Lambda^\circ p$ bound state has been observed.[6] However, in $K^- d \to \pi^- \Lambda^\circ p$ a very strong, narrow enhancement in the $\Lambda^\circ p$ mass spectrum has been observed at 2129 MeV.[7-9] It is most likely in the ^3S state. We have plotted this in Fig. 6 for comparison with our values of $\alpha(t)$. It could represent a bound state of the Σp or Σn system, or perhaps a cusp effect at the Σ-nucleon threshold. It is interesting to note that some recent bag model calculations can accomodate a six-quark state with these quantum numbers in this mass range.[10] The slope, α', of $\alpha(t)$ vs. t is not sufficiently constrained by our data alone to distinguish between the exchange of a single Reggeon ($\alpha' \simeq 1$), and a cut contribution from a two-Reggeon system ($\alpha' \approx 0.5$). If the $\Lambda p(2129)$ is included as a constraint, then single-Reggeon exchange is favored.

We have confined ourselves to purely qualitative remarks here because of possible systematic errors in the extrapolation of the $\bar{\Lambda}^\circ$ production data into the triple Regge region.

On general grounds, it is possible to express the polarization, P, of lambdas inclusively produced by protons as

$$P = \frac{2 \sin \theta^* \, \mathrm{Im}(f^* g)}{|f|^2 + |g|^2 \sin^2 \theta^*} \tag{4}$$

where θ^* is the c.m. production angle and f (g sin θ) is the non-flip (spin-flip) amplitude analogous to that in elastic scattering. In our case, $\sin^2 \theta^* < 0.06$. We set $g/f = r\, e^{i\psi}$. If r is of order unity or less, then $P \approx 2\, r \sin \theta^* \sin \psi$.

Using our polarization data[1], we have studied the quantity $P/\sin \theta^*$ over the same range as the lambda production cross sections, $0.5 < x < 1.0$, and $0 < -t < 5\ \mathrm{GeV}^2$. We find $k\ \alpha\ P/\sin \theta^* =$ constant $= 0.94 \pm 0.14$ ($\chi^2 = 19$ for 21 d.f.) where $\alpha = 0.647 \pm 0.013$ is the asymmetry parameter in lambda decay, and k is a dilution factor to account for secondary lambdas resulting from the decay $\Sigma^\circ \to \Lambda^\circ \gamma$. We estimate $k = 0.75 \pm 0.08$, where this accounts for the estimated $\Sigma^\circ/\Lambda^\circ$ production ratio and a range of Σ° polarization from equal to opposite that of the Λ°. Thus, $P/\sin \theta^* = 1.93 \pm 0.36$, and $r \sin \psi = 0.96 \pm 0.18$, independent of x and t. Of the many interpretations, an interesting possibility is that f and g are roughly equal and 90° out of phase. From our earlier discussion, $|f|^2 + |g|^2 \sin^2\theta^*$ seems to be related to K* and K** exchange diagrams as shown in Fig. 2(b-c). The most obvious candidate for the interference term, 2 Im (f*g) sin θ^*,

in a triple-Regge model is a diagram of the type shown in Fig. 2f.[(a)] The amplitudes can be related to various spin-dependent residue functions from the triple-Regge diagrams.[12,13] If the three diagrams discussed so far are the only important ones, then the model predicts the same x-dependence for all of them, and the polarization, which involves only the ratio, should be independent of x as is observed. The t-dependence of the residue functions is not a prediction of the model. The approximate t-independence of the observed polarization suggests that, within a constant factor, the various residue functions have the same t-dependence.

It has been argued that, if the Pomeron is an SU(3) singlet, then the K* K** Pomeron diagram of Fig. 2f does not exist and cannot be the source of the Λ° polarization.[12] The existence of strong, perhaps maximal, polarization suggests the possibility of an antisymmetric octet contribution of the Pomeron. There is evidence for its having symmetric octet behavior,[14-16] but prior to our experiment none has been available for or against antisymmetric octet behavior. Another possibility is that the polarization results from absorptive corrections to the triple-Regge diagrams. Calculations[17,18] show polarization but do not fully reproduce our data.

Whether or not the triple-Regge model has any deep fundamental significance, it appears to be a useful and orderly framework for

[(a)] If α_3 = Pomeron, the polarization should scale. Polarization has been observed in Λ° production by 28 GeV protons. It has the same p_T dependence as the 300 GeV results of Ref. 1 within available accuracy.[11]

representing inclusive data. In this context, it has predictive power and we suggest one example. The production of neutral strange particles by pions should be governed by diagrams similar to those we have discussed. The process $\pi N \rightarrow K_s^\circ X$ should involve K* and K** exchange in diagrams similar to those of Fig. 2(b-c). The production cross sections should show kinematic behavior like that of Fig. 1(a). At high x, the production of Λ° and $\bar{\Lambda}^\circ$ should be identical, governed by diagrams similar to Fig. 2(d), and show kinematic behavior like that of Fig. 1(b). Preliminary analysis of our data on production of Λ°, $\bar{\Lambda}^\circ$ and K_s° by pions tends to confirm these predictions.

We are pleased to acknowledge the important contributions of the staff at Fermilab in obtaining these data. Additional thanks are due to the Center for Computer and Information Services at Rutgers for facilities used in this analysis. One of us, (T.D.) is grateful to T. F. Wong, R. D. Field and C. Quigg for helpful conversations.

REFERENCES AND FOOTNOTES

* Present Address: Argonne National Laboratory, Argonne, Illinois, 60439

† Present Address: Brookhaven National Laboratory, Upton, Long Island, N. Y. 11973

‡ Work supported in part by the National Science Foundation.

†† Work supported in part by the U. S. Energy Research and Development Administration.

1. G. Bunce et al., Phys. Rev. Letters 36 (1976) 1113.
2. P. Skubic et al. (to be submitted to Physical Review).
3. R. D. Field and G. C. Fox, Nucl. Phys. B80 (1974) 367.
4. V. Blobel et al., Nucl. Phys. B69 (1974) 367.
5. K. Alpgard et al., Nucl. Phys. B105 (1976) 349.
6. A. Gal, Advances in Nuclear Physics 8 (1975) 1.
7. D. Cline, R. Laumann, J. Mapp, Phys. Rev. Letters 20 (1968) 1452.
8. G. Alexander, et al., Phys. Rev. Letters 22 (1969) 483.
9. T. H. Tan, Phys. Rev. Letters 23 (1969) 395.
10. R. Jaffe (private communication).
11. K. Heller, et al. (to be published).
12. R. D. Field, Calif. Inst. of Technology Report CALT-69-459.
13. G. Goldstein and J. Owens, Nucl. Phys. B103 (1976) 145.
14. P. R. Stevens, G. F. Chew and C. Rosenzweig, Nucl. Phys. B110 (1976) 355.
15. C. Quigg and E. Rabinovici, Phys. Rev. D13 (1976) 2525.

16. J. Pumplin and G. Kane, Phys. Rev. D11 (1975) 1183.

17. F. E. Paige and D. P. Sidhu, Phys. Rev. D14 (1976) 2307.

18. K. J. M. Moriarty et al., Nuovo Cimento Letters 17 (1976) 366.

FIGURE CAPTIONS

Fig. 1 Inclusive production of Λ°, K_s° and $\bar{\Lambda}^\circ$ by 300 GeV protons on beryllium. The lines are the result of fitting procedures described in the text.

Fig. 2 Triple-Regge diagrams for the general inclusive process $a + b \to c$ + anything, and for specific processes discussed in the text.

Fig. 3 The data of Fig. 1(a) interpolated to give the (1-x) dependence at several fixed-t values.

Fig. 4 Values of the Regge parameter $\alpha(t)$ from fits to Λ° production plotted vs. t. The s-channel states K*(890), K**(1420) and K(494) are shown for comparison.

Fig. 5 Values of the Regge parameter $\alpha(t)$ from fits to K_s° production plotted vs. t. A number of possibly-related s-channel Σ states are shown for comparison.

Fig. 6 Values of the Regge parameter $\alpha(t)$ from fits to $\bar{\Lambda}^\circ$ production plotted vs. t. An enhancement in the Λp mass spectrum observed at 2129 MeV in $K^- d \to \pi^- \Lambda p$ is shown for comparison under the assumption that it is a ^3S state.

TABLE 1. Triple-Regge Parameters Fitted to Inclusive Production Cross Sections[a]

Process	θ_i	t_i (GeV^2)	$\alpha(t_i)$	$\beta(t_i)$ (mb/GeV^2)	χ^2/D.F.
$pN \to \Lambda^\circ X$	0.6	-0.04	+0.19 ± 0.02	1.94 ± 0.08	44.4/44
	1.4	-0.19	+0.08 ± 0.02	1.87 ± 0.08	
	3.1	-0.85	-0.47 ± 0.02	2.01 ± 0.11	
	5.0	-2.19	-1.28 ± 0.05	1.64 ± 0.17	
	7.1	-4.40	-2.48 ± 0.19	2.33 ± 0.79	
	8.9	-6.91	-4.23 ± 0.53	6.48 ± 8.11	
$pN \to K_s^\circ X$	0.6	-0.01	-1.21 ± 0.09	1.47 ± 0.22	37.6/38
	1.4	-0.15	-1.30 ± 0.10	1.51 ± 0.24	
	3.1	-0.81	-2.10 ± 0.13	2.01 ± 0.38	
	5.0	-2.16	-3.05 ± 0.18	2.47 ± 0.60	
	7.1	-4.36	-4.03 ± 0.58	2.58 ± 1.86	
	8.9	-6.87	-6.11 ± 0.51	9.38 ± 4.07	
$pp \to \bar{\Lambda}^\circ X$	0.6	-0.04	-3.87 ± 0.79	1.05 ± 0.65	11.0/14
	1.4	-0.19	-3.18 ± 0.76	0.45 ± 0.28	
	3.1	-0.85	-4.11 ± 0.97	0.87 ± 0.65	
	5.0	-2.19	-4.72 ± 0.78	0.80 ± 0.50	
	7.1	-4.40	-6.16 ± 0.68	1.33 ± 0.66	
	8.9	-6.91	-7.85 ± 0.54	2.68 ± 1.01	

[a] Single-nucleon cross sections obtained by extrapolating those from Be, Cu and Pb to A = 1.

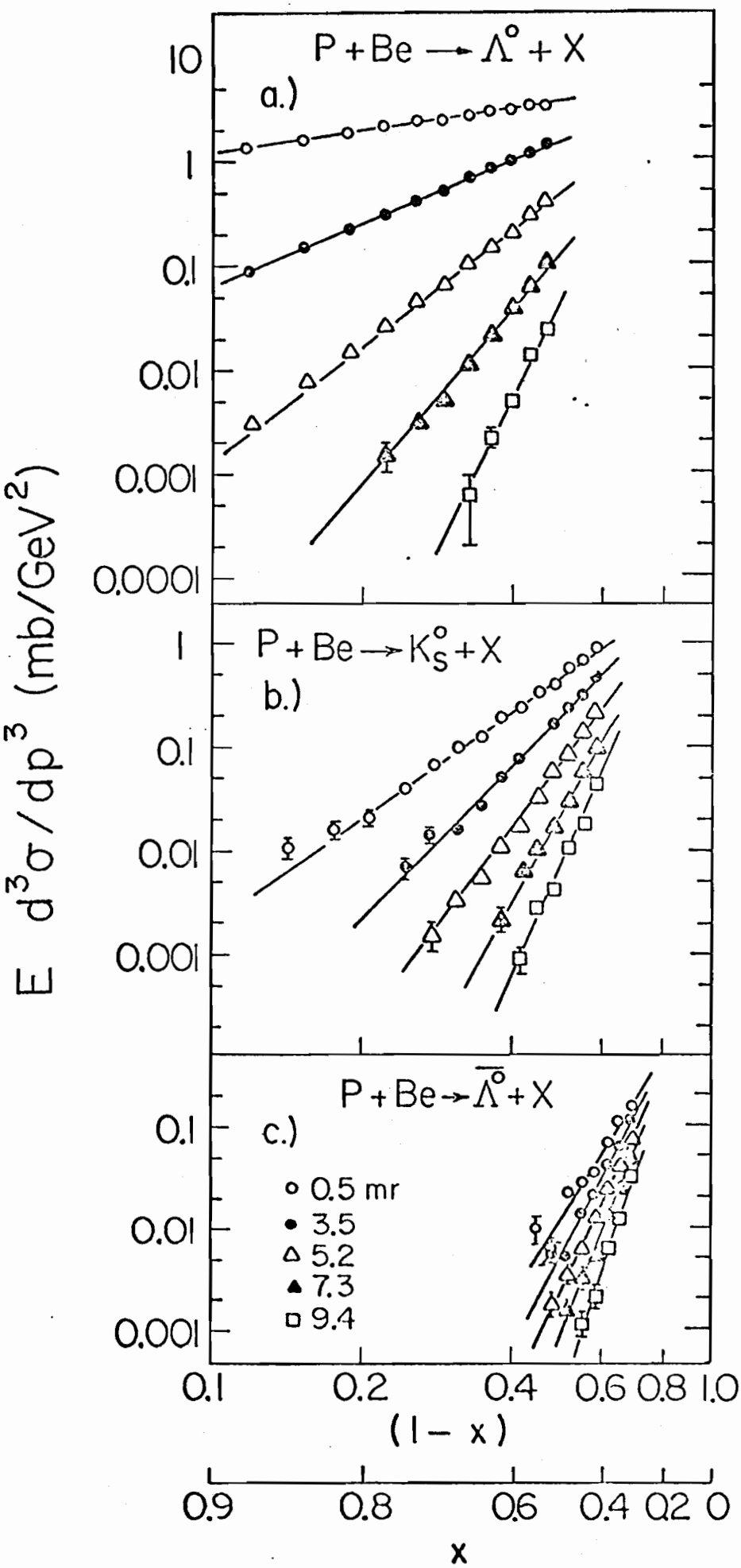
P + Be → Λ° + X
a.)
P + Be → K°S + X
b.)
P + Be → Λ̄° + X
c.)
0.5 mr
3.5
5.2
7.3
9.4
E d³σ/dp³ (mb/GeV²)
10
1
0.1
0.01
0.001
0.0001
0.1
0.2
0.4
0.6
0.8
1.0
(1 − x)
0.9
0.8
0.6
0.4
0.2
0
x

Fig 1

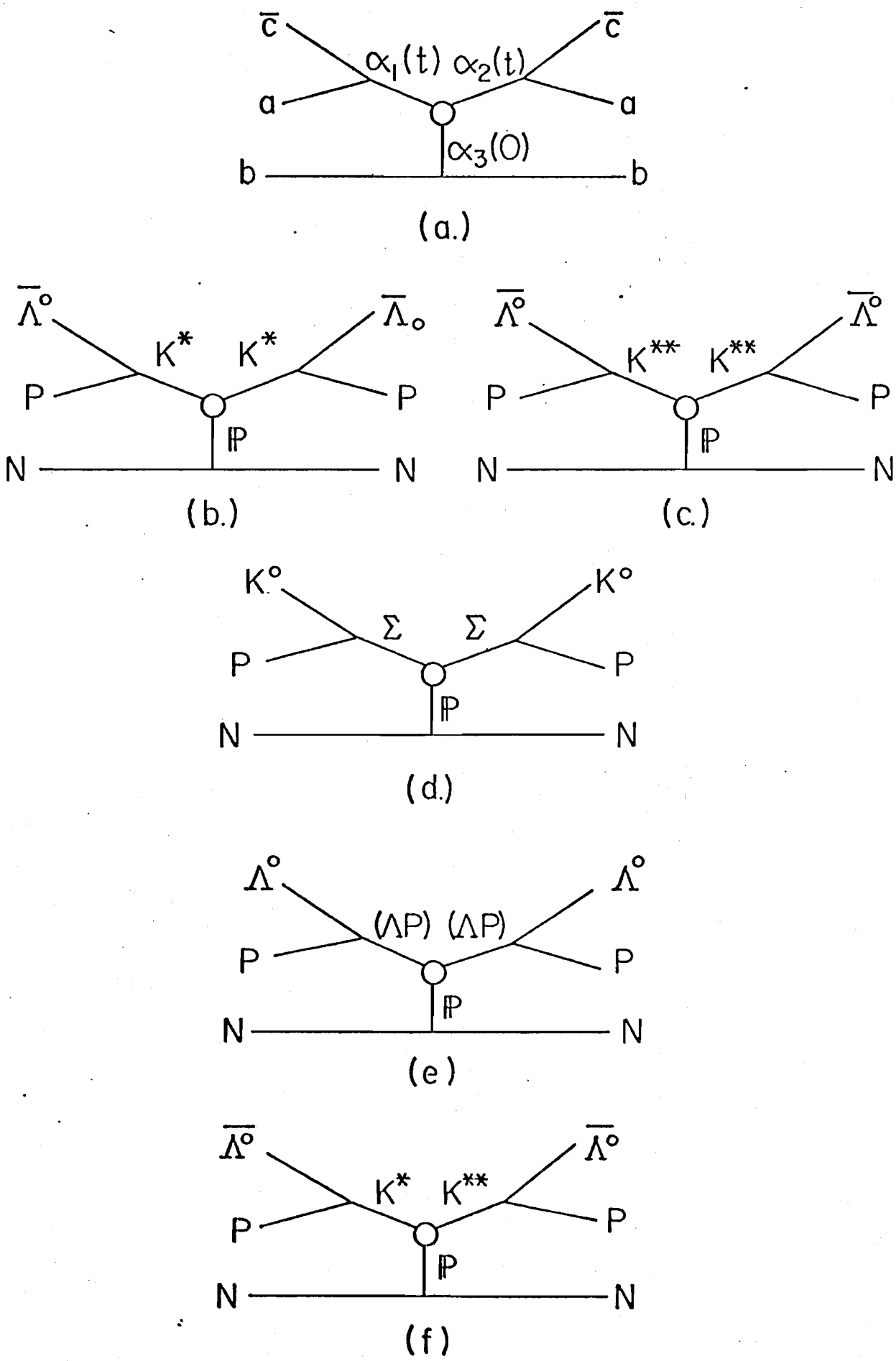
c̄
c̄
α1(t) α2(t)
a
a
α3(0)
b
b
(a.)
Λ̄°
Λ̄°
K*
K*
P
P
ℙ
N
N
(b.)
Λ̄°
Λ̄°
K**
K**
P
P
ℙ
N
N
(c.)
K°
K°
Σ
Σ
P
P
ℙ
N
N
(d.)
Λ°
Λ°
(ΛP) (ΛP)
P
P
ℙ
N
N
(e)
Λ̄°
Λ̄°
K*
K**
P
P
ℙ
N
N
(f)

Fig. 2.

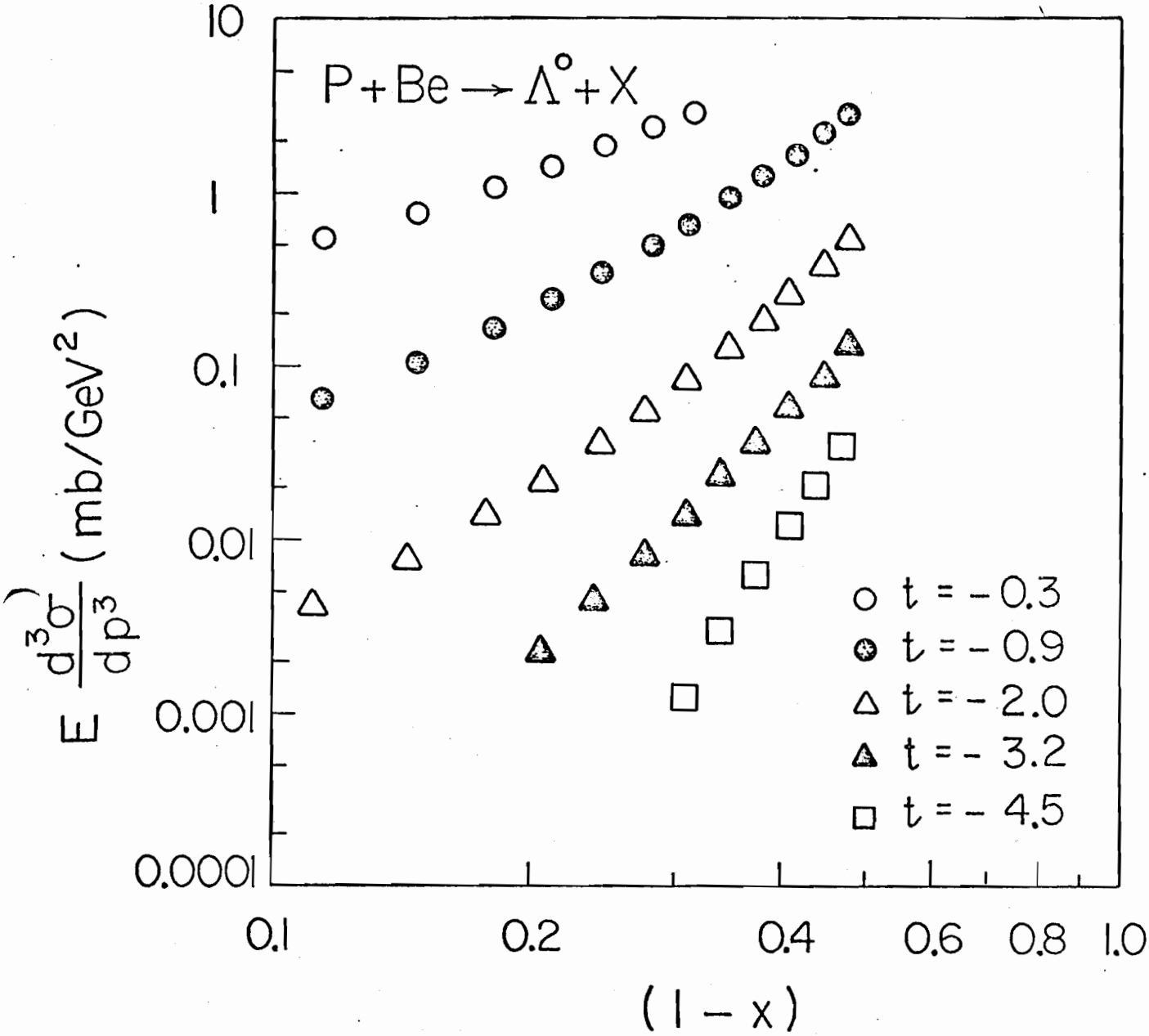
P + Be → Λ° + X
10
1
0.1
0.01
0.001
0.0001
E d³σ/dp³ (mb/GeV²)
0.1
0.2
0.4
0.6
0.8
1.0
(1 − x)
t = −0.3
t = −0.9
t = −2.0
t = −3.2
t = −4.5

Fig. 3.

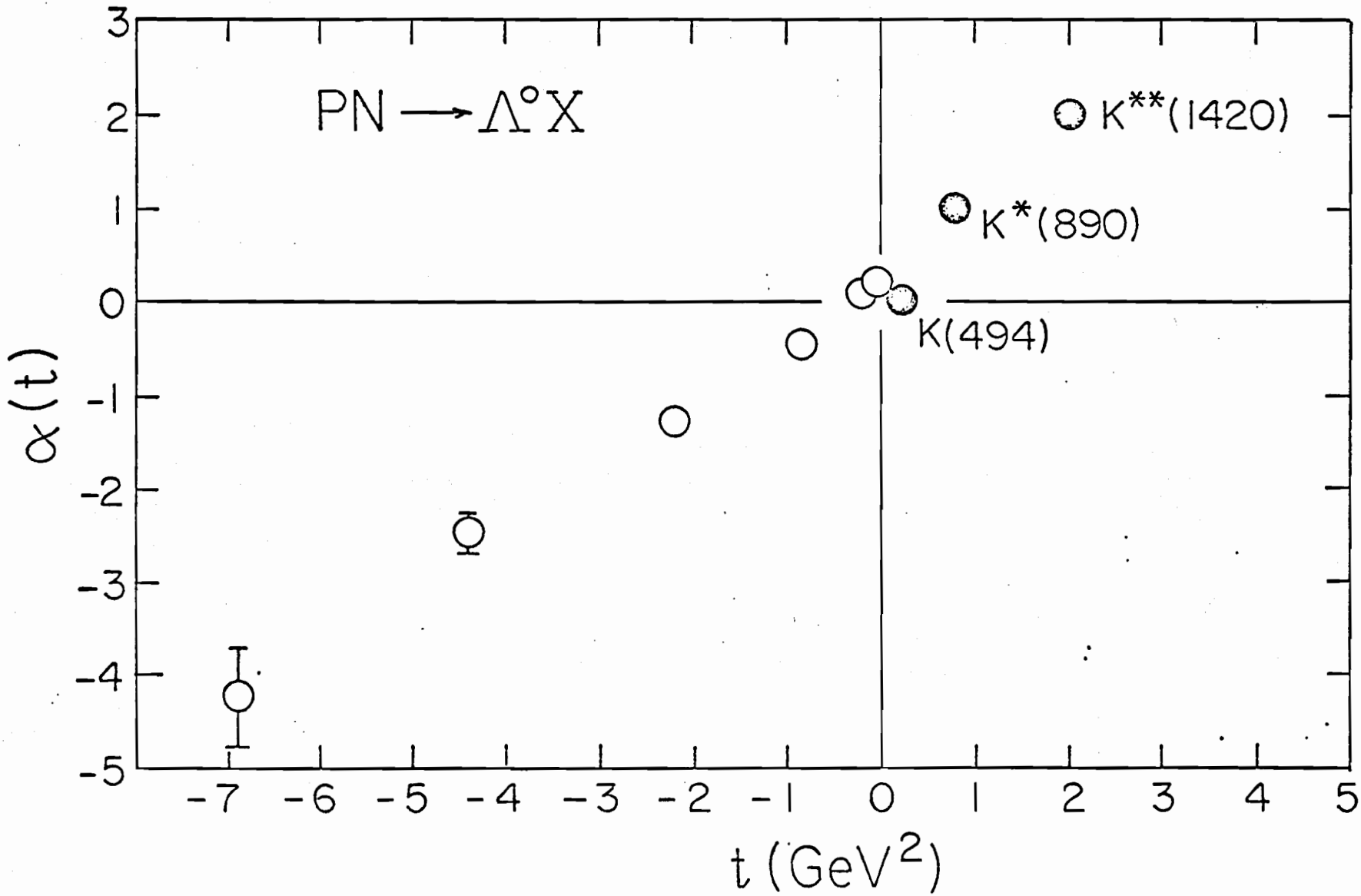

Fig. 4.

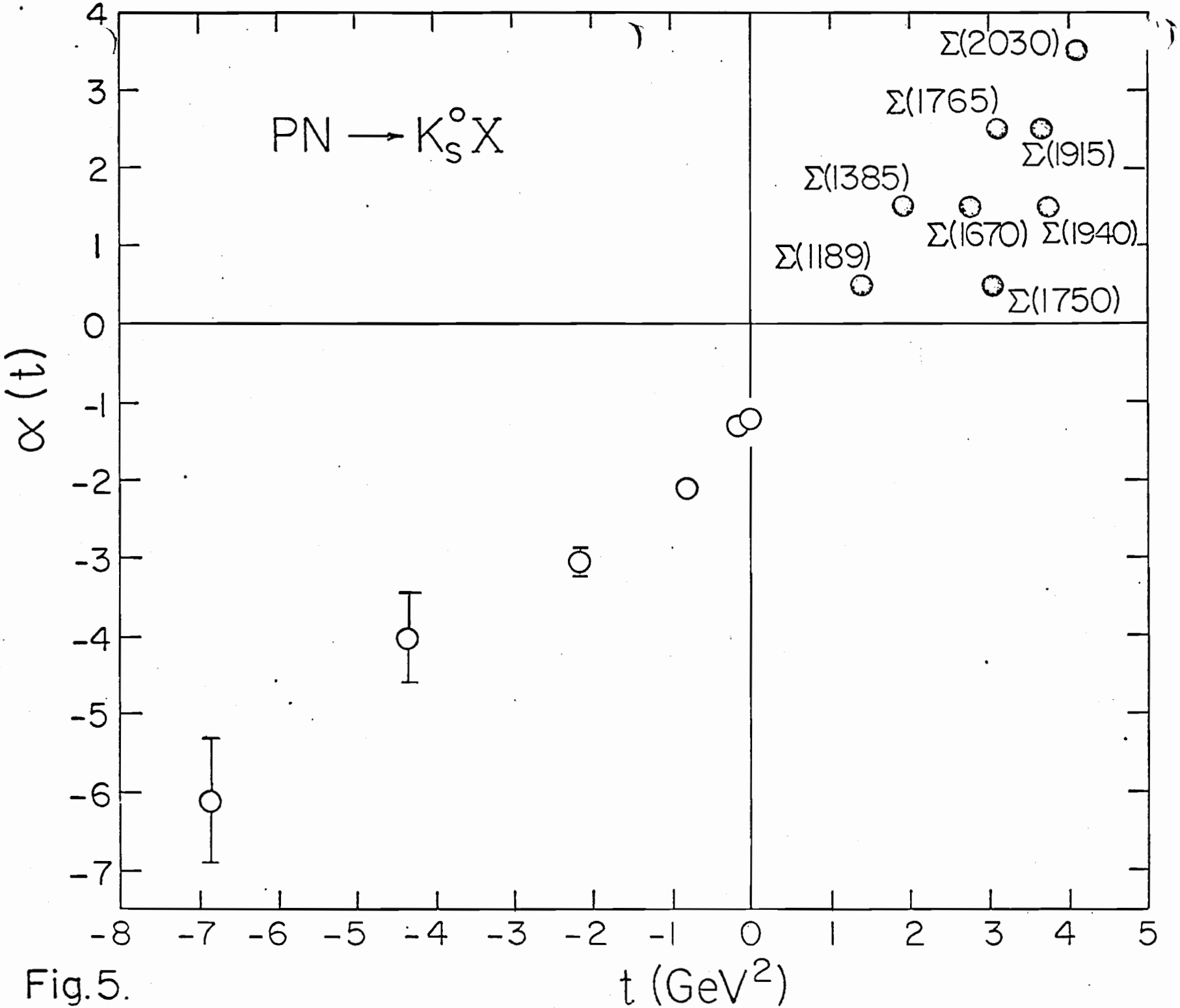
PN → K_S^0X
Σ(2030)
Σ(1765)
Σ(1915)
Σ(1385)
Σ(1670)
Σ(1940)
Σ(1189)
Σ(1750)
α(t)
t (GeV²)
4
3
2
1
0
-1
-2
-3
-4
-5
-6
-7
-8
-7
-6
-5
-4
-3
-2
-1
0
1
2
3
4
5

Fig.5.

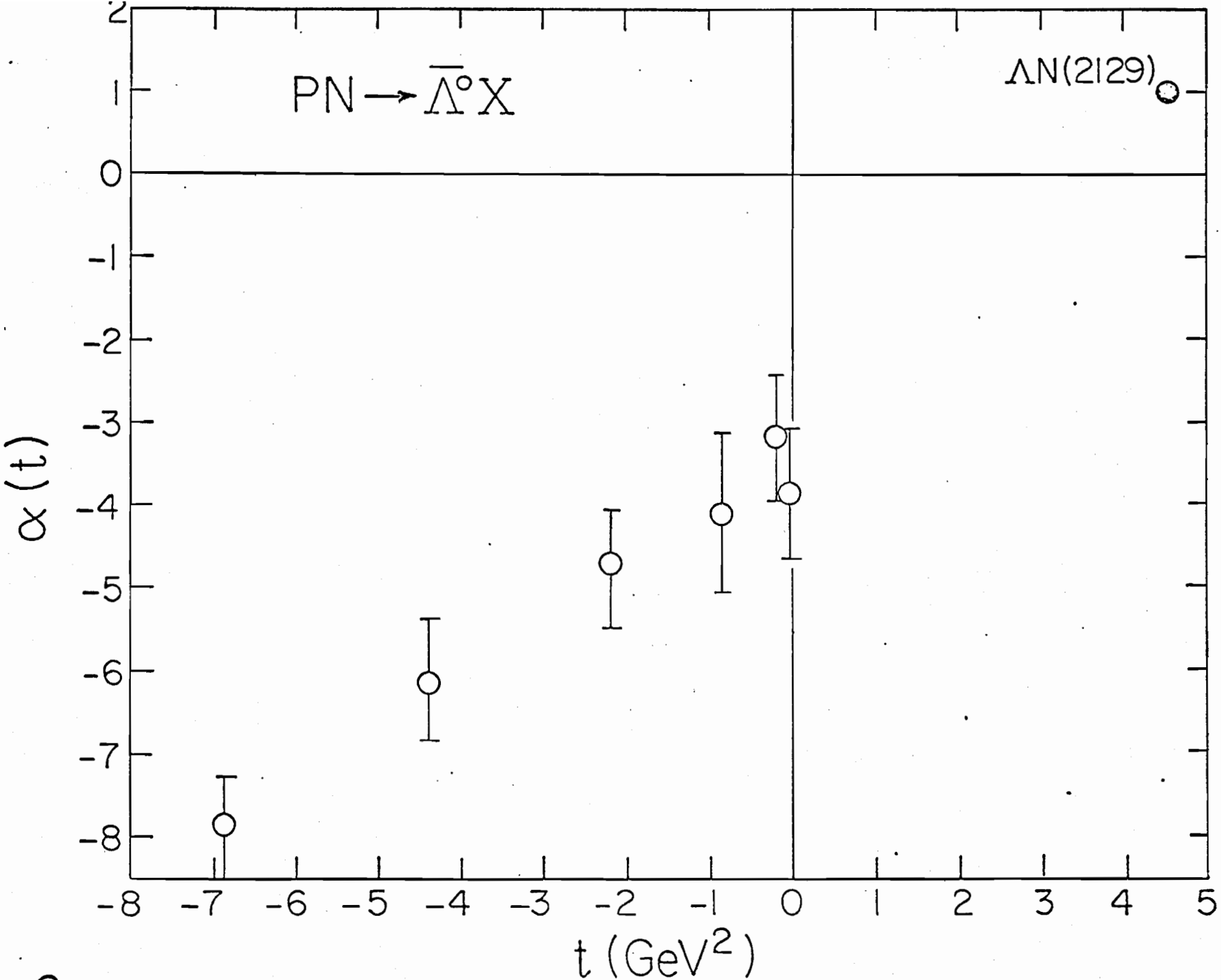
PN → $\bar{\Lambda}^{o}$X
ΛN(2129)
α(t)
t (GeV^2)
2
1
0
-1
-2
-3
-4
-5
-6
-7
-8
-8
-7
-6
-5
-4
-3
-2
-1
0
1
2
3
4
5

Fig. 6.